frontiers | Frontiers in Marine Science

TYPE Original Research
PUBLISHED 03 September 2024
DOI 10.3389/fmars.2024.1469307

OPEN ACCESS

EDITED BY
Yang Yang,
Nanjing Normal University, China

REVIEWED BY
Haifei Yang,
East China Normal University, China
Junbiao Tu,
Tongji University, China
Chao Gao,
Nanjing University, China

*CORRESPONDENCE
Zeng Zhou
zeng.zhou@hhu.edu.cn

RECEIVED 23 July 2024
ACCEPTED 15 August 2024
PUBLISHED 03 September 2024

CITATION
Chen L, Moeller I, Zhou Z, Hu Z, Zhang Y, Chu M, Jia Y, Townend I and Zhang C (2024) Seasonal biophysical interactions in tidal marsh evolution: insights from a synchronized dataset in Jiangsu, China. *Front. Mar. Sci.* 11:1469307. doi: 10.3389/fmars.2024.1469307

Seasonal biophysical interactions in tidal marsh evolution: insights from a synchronized dataset in Jiangsu, China

Lei Chen[1], Iris Moeller[2], Zeng Zhou[1,3]*, Zhan Hu[4], Yanan Zhang[5], Mengwei Chu[5], Yifei Jia[6], Ian Townend[7] and Changkuan Zhang[1]

[1]The National Key Laboratory of Water Disaster Prevention, Hohai University, Nanjing, China, [2]Department of Geography, Trinity College Dublin, Dublin, Ireland, [3]Jiangsu Key Laboratory of Coastal Ocean Resources Development and Environment Security, Hohai University, Nanjing, China, [4]School of Marine Sciences, Sun Yat-sen University, Zhuhai, China, [5]Yancheng Wetland and World Natural Heritage Protection Management Center, Yancheng, China, [6]School of Ecology and Nature Conservation, Beijing Forestry University, Beijing, China, [7]School of Ocean and Earth Sciences, University of Southampton, Southampton, United Kingdom

Introduction: Tidal marsh wetlands provide essential and valuable services to the wider interconnected marine and coastal environment, although the complex intertwined processes in morphological evolution remain insufficiently understood owing to synchronized data scarcity, limiting the development of numerical models and management strategies.

Methods: This study investigated the hydrodynamic, biological, sediment and morphological processes on the Doulong tidal wetlands, Jiangsu, China, using a one-year field dataset that captured spatial and seasonal variations.

Results and discussion: Our results indicate that biophysical interactions among multiple processes could result in some overlooked sedimentary behaviours and bio-morphological patterns in tidal marsh wetlands. Firstly, the dominance of alongshore currents caused a rapid alongshore expansion of saltmarsh patches, by which the marsh edge achieved seaward advancing, markedly different from the widely reported cross-shore expansion. Secondly, results showed that the particle size of sediment near the marsh edge coarsened when plants withered and then fined when plants grew, indicating that the seasonal variation trend of sediment grain size in saltmarshes was opposite to the trend of vegetation biomass. Thirdly, the interaction between vegetation and stranded marine debris formed banded debris zones within the saltmarsh, where debris bands could cause a biomass reduction of up to 58%, disrupting the commonly-observed parabolic biomass-elevation relationship. Meanwhile, the seasonal variation of vegetation and hydrodynamics could alter the debris positions and hence result in the formation of multiple parallel debris bands. Overall, this study

provides a synchronized dataset and elucidates specific bio-morphological relationships and processes that have thus far not been systematically documented, enhancing the comprehensive understanding of tidal marsh wetland evolution.

KEYWORDS

synchronized, seasonal, morphodynamics, alongshore expansion, biomass, marine debris

1 Introduction

Tidal marsh wetlands, among one of the most productive and biologically diverse ecosystems, provide valuable ecosystem services, such as nutrient cycling, carbon storage, and habitat provision (Barbier et al., 2011; Mudd and Fagherazzi, 2016; Nahlik and Fennessy, 2016; Li et al., 2022). Meanwhile, they have drawn widespread attention due to their coastal protection function and potential land resources (Zhou et al., 2022a). As is the case for other coastal depositional landforms, tidal wetlands are naturally dynamic, however, due to climate change, sea level rise, human activities, and the lack of adaptive management measures, marsh wetlands are facing degradation and loss (Spencer et al., 2016; Wu et al., 2017; Li et al., 2018; Chen et al., 2020a; Pannozzo et al., 2021). Thus, understanding the morphodynamics, particularly the longshore and seaward expansion or erosion of tidal marsh wetlands is essential for their conservation and restoration.

As the buffer zone between land and sea, tidal marsh wetlands are highly dynamic and heterogeneous (van de Koppel et al., 2005; Li et al., 2019, 2021; Houttuijn Bloemendaal et al., 2021). The early relevant research predominantly focused on either physical aspects, such as hydrodynamics and sediment transport, or biological aspects, such as vegetation dynamics and species diversity. These approaches have significantly advanced our understanding of tidal marsh functioning, but the isolated understanding of physical or biological processes alone is insufficient to accurately elucidate the evolutionary mechanisms of tidal marsh wetlands because biophysical interactions play a crucial role. Field observations suggest that vegetation can significantly attenuate tidal currents and waves related to plant characteristics (Möller, 2006; Möller et al., 2014; Cao et al., 2021; Evans et al., 2022; Wei et al., 2022). Correspondingly, plant growth in different environments depends on hydrodynamics and landscape (Fraaije et al., 2015; Chen et al., 2020b). Numerical models have also attempted to consider the impacts of vegetation on estuarine and coastal morphodynamics (Zhou et al., 2016; Best et al., 2018), but our knowledge of biophysical relationships remains inadequate due to the limited availability of synchronized biophysical field measurements.

In addition to the need for synchronized data, the unique morphological patterns in tidal flats cannot be ignored. For example, most studies on saltmarsh evolution have primarily focused on cross-shore processes, particularly in modelling research (Zhou et al., 2016; Zhao et al., 2017; van der Wal et al., 2023). There is a lack of how wetland evolution might be connected to alongshore currents, sediment transport and vegetation on open coasts. Besides, as marine debris is becoming more common (Thiel et al., 2013; Browne et al., 2015), its intrusion into the wetland system during spring tides and storm events and retention during neap tides, can be a potentially important biogeomorphological process control (Viehman et al., 2011). Although vegetation plays an important role in capturing marine debris, the shrubby nature of the salt marsh vegetation can trap such debris for prolonged periods, ultimately leading to negative impacts on the growth of vegetation (Uhrin and Schellinger, 2011; Corbau et al., 2023). However, there is limited research on the distribution and impacts of marine debris in saltmarsh areas.

This study provides a biogeomorphological field dataset from the tidal marsh wetland on the central Jiangsu coast, China, to address the following specific scientific objectives: (1) The differences between the alongshore and cross-shore expansion pattern of saltmarsh patches; (2) The seasonal distribution and variation characteristics of vegetation biomass and sediment grain size; (3) The impact of marine debris on saltmarsh vegetation biomass and its movement characteristics. By addressing these objectives, this study emphasizes the importance of synchronous biogeomorphological observations when working towards better prediction of coastal wetland change and thus a pro-active approach towards the sustainable management of coastal wetlands.

2 Materials and methods

2.1 Study area

Field observations were conducted on the intertidal flat of Doulong, the central region of the Jiangsu coast, China (Figure 1A). The Jiangsu coast is located between the abandoned Yellow River Delta and the Yangtze Estuary, with a total length of 954 km. Since the Jiangsu coast is jointly influenced by fluvial and marine forcing, the coastal environment is dynamic and characterized by spatio-temporal morphological variations. The nearshore tides in the study area are irregular semidiurnal, with a tidal range of 2.56 m on average and 3.40

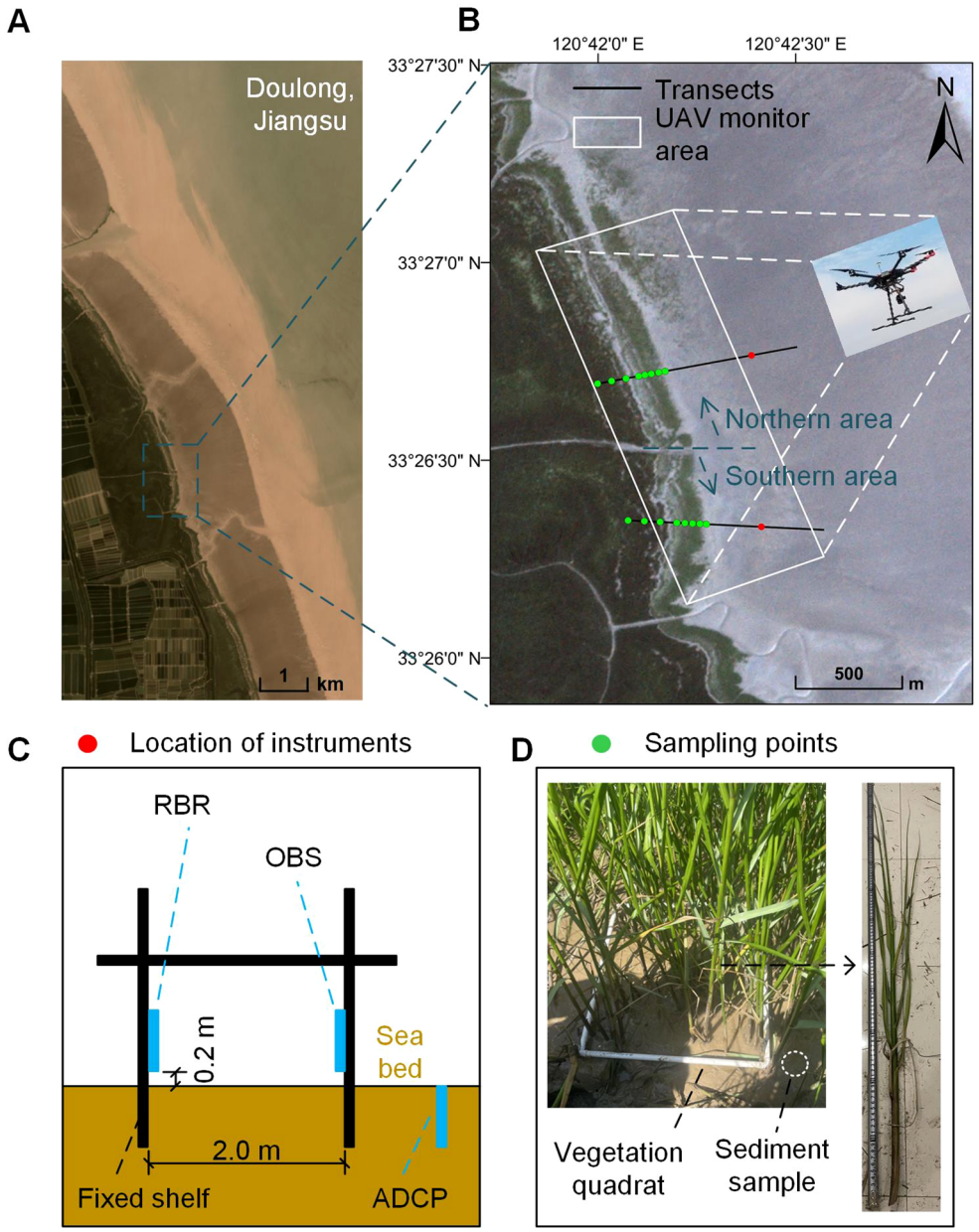

FIGURE 1
The location of the study area **(A)** and an overview of the area and transects covered in the study **(B)**. Sketch of the physical measurement station **(C)** and vegetation and sediment sampling **(D)**. Source of aerial images: © Planet Explorer.

m during spring tides (data from Xinyanggang gauging station). The overall evolution of the Jiangsu coast shows a pattern of erosion in the north and accretion in the south (Chen et al., 2020b). In the northern part of this study area is the Yancheng Wetland National Nature Reserve. For nature conservation within the protected area, the adjacent regions of the reserve are restricted from large-scale human activities. Therefore, the observed saltmarsh in this study can be recognized as a natural environment without intensive direct human intervention. In 1982, *Spartina alterniflora* was introduced to the Jiangsu coast because of its positive effects on sediment trapping and coastal protection (Chung et al., 2004; Gao et al., 2014), and then spread rapidly due to its strong adaptability and competitiveness (Zhang et al., 2004). *Spartina alterniflora* has replaced the native species *Suaeda salsa* as the dominant marsh community in the study area. Recently, China has started to control and manage *Spartina alterniflora*, but there was no human intervention during this observation period.

The marsh edges in the Doulong region represent cliffs and smooth transitions. Zhao et al. (2017) observed the rapid formation of marsh-edge cliffs in the Yancheng Nature Reserve core region over a period of only some 5 years. Chen et al., (2020b) observed three different features of the saltmarsh edge on the Doulong tidal flat, including marsh-edge cliffs, marsh patches, and the coexistence of cliffs and patches.

To explore the seasonal changes in vegetation, hydrology and morphology, measuring and sampling were undertaken in 2020.09.19, 2020.12.09, 2021.03.15, and 2021.07.16, which represented autumn,

winter, spring, and summer, respectively. Four observation periods were all during neap tides. The wind speed data during observation periods was obtained from a nearby monitor station (Supplementary Table 1). Based on the 8-day average wind speed, the wind speed in July 2021 was highest (4.356 m/s) and in September 2020 was lowest (2.112 m/s). Although the wind conditions were not similar during the four observation periods, the seasonal variations in wind conditions could be partially reflected in the hydrodynamic results.

2.2 UAV photography

Remote sensing images have been used to capture the kilometer-scale morphological evolution, but existing data provides insufficient temporal and spatial resolution data to resolve seasonal-to-annual dynamics (Frazier and Page, 2000; Marani et al., 2006; Yang et al., 2019). UAV (Unoccupied Aerial Vehicle) observation technology has been widely used to obtain information on kilometer-scale and seasonal-to-annual resolution landscape evolution (Moffett et al., 2015; Dai et al., 2021; Chen et al., 2022). Therefore, in this study, a rectangular UAV monitoring zone was established at the marsh margin where the evolution of features such as marsh-edge cliffs, marsh patches and tidal creeks were most evident.

A DJI MATRICE 600 UAV was employed for the aerial field surveys. The UAV was equipped with a ZENMUSE X5 16.0 MP camera (Figure 1B). The same observation range and flight route were set every time when the site was resurveyed. The observation domain was approximability 1.5 km × 0.5 km, covering the marsh edges, tidal creeks and frontal marsh patches. The flight altitude was 80 m and the overlap rate of the images along the parallel or perpendicular direction to the flight direction was 50%. These parameters were selected to optimize the coverage of the observation area, endurance of the drone, and image quality. The *Agisoft PhotoScan* software was used to process the images with acquired GPS information. After aligning photos, establishing the dense point cloud and constructing the mesh, georeferenced orthoimages were generated. In this study, three drone flights were conducted in December 2020, March 2021, and July 2021, collecting a total of 1854 photos. These photos were processed into three orthophotos showing the topography of the saltmarsh in different seasons.

2.3 Hydrodynamic measurements

The observation area was divided into northern and southern zones, with the cross-shore channel in the middle as a reference (Figure 1B). To obtain changes in variables along the cross-shore direction, two transects (transect S and transect N) were set in the northern and southern zones. Due to the movement of the marsh edge and the rapid development of marsh patches, it was challenging to establish a long-term observation site within the saltmarsh. Therefore, two hydrodynamic observation sites were ultimately set up on the unvegetated flat with a distance of approximately 500 meters. *In-situ* measurements (see below) were conducted at each site to allow a comparison between the northern and southern zones (Figure 1B).

A self-made shelf fixed with 4 anchors was used to install the instruments safely and firmly at each site (Figure 1C). All instruments were self-contained and set up in advance. Water levels and waves were recorded by a tide and wave logger (RBR), installed 20 centimeters above the sea bed, and set to record every 20 minutes with a frequency of 4 Hz for 4096 wave burst samples. An optical backscatter sensor (OBS-3A) was attached to the shelf at a height of 20 centimeters above the bed to monitor suspended sediment concentration (SSC), which was set up in cyclic configuration at 1 Hz with an interval of 150 seconds. An Acoustic Doppler Current Profiler (ADCP) was deployed in an up-looking configuration at 2 MHz with an interval of 150 seconds to extract the velocity profile.

2.4 Bathymetry observation and sample collection

Topographic change along the transects was measured by Real-Time Kinematic (RTK) dGPS instruments with an accuracy of 15 mm in the vertical and 10 mm in the horizontal. On the *S. alterniflora* marsh area, 8 vegetation sampling points were selected along each transect to be representative of the specific general cross-shore surface cover type in the vicinity (Figure 1D). The spacing between the four points closer to the edge was approximately 20 m, while the spacing between the four more landward points was approximately 50 m. Surface sediment samples (upper 2–3 cm in depth) were collected at the same points to determine the median bed sediment grain size (D_{50}), with 8 samples from each transect in each season.

Each plant sample was a 0.5 m × 0.5 m quadrat, marked by a PVC frame. The harvested plant samples were dried in a 90 ° oven for 12 hours until they reached a stable dry weight, which is the above-ground dry biomass. The grain size of the surface sediment was measured using a laser particle size analyzer (Malvern 3000).

3 Results

In this study, the evolution of several morphological patterns could be clearly observed using the UAV orthoimages, including marsh-edge cliffs, marsh patches and channels, and even some bands of stranded marine debris and unvegetated zones. The transect data showed the detailed cross-shore distribution of bed level, vegetation biomass and sediment. The on-site sensors recorded the representative hydrodynamic data of the study area.

3.1 Evolutions of morphological patterns

In December 2020, the most prominent observation was the large extent of marsh patches in the northern area, with the farthest cluster located approximately 150 meters from the marsh edge (Figure 2A). There was a tidal channel in the north surrounded by dense marsh patches, which extended toward the south. In contrast, in the southern area, there were only a few patches near the marsh margin. There was also a tidal channel extending toward the north. The outline of the marsh edge exhibited an irregular and jagged pattern. In March 2021,

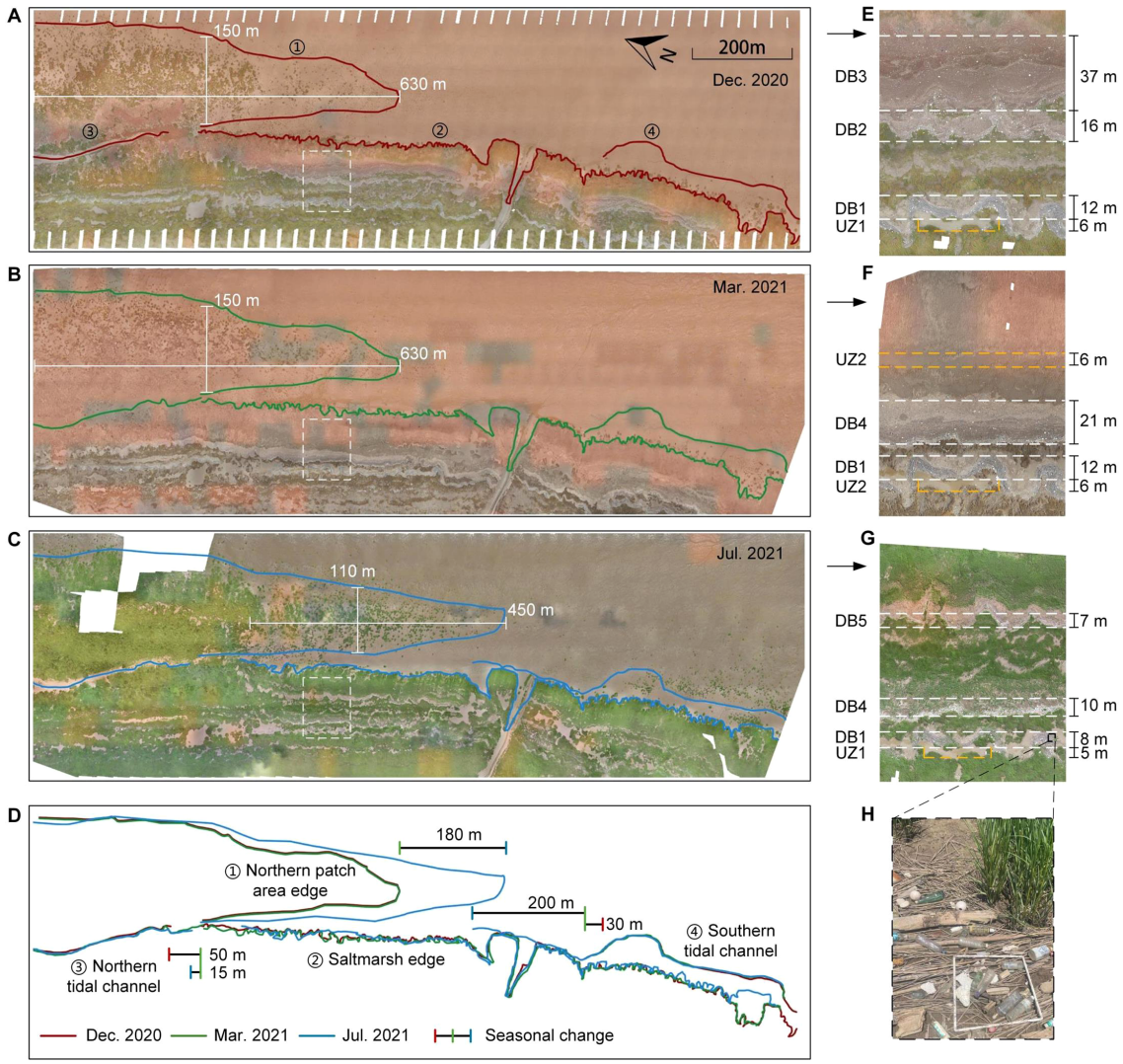

FIGURE 2
The UAV orthoimages of the tidal flat at Doulong Harbor in **(A)** December 2020, **(B)** March 2021 and **(C)** July 2021. **(D)** showed the outlines of morphological patterns. The white and yellow dashed boxes, magnified in **(E)**, **(F)** and **(G)**, showed the evolution of the debris bands (DB) and unvegetated zones (UZ). **(H)** showed the common debris.

the northern patch area became sparser because the above-ground part of the *Spartina* plant was withered during winter (Figure 2B). The northern channel head extended southward by 50 meters and the southern channel extended by 30 meters (Figure 2D). The marsh edge experienced slight erosion and retreated. In July 2021, the northern patch area showed noticeable changes, with its boundary extending southward by around 180 meters compared to March 2021. Moreover, the original patches had almost interconnected together and became part of the marshland (Figure 2C). Because of this change, the northern channel head was obstructed by vegetation, hindering its southward expansion, and even retreated by 15 meters compared to March 2021. However, the southern tidal channel head continued to extend northward by around 200 meters. Vegetation patches started to emerge on both sides of the southern channel as part of an expansion of the southern marsh edge (Figure 2D).

Two distinct morphological patterns were observed within the saltmarsh: the debris bands and the bare/unvegetated zones (Figure 2). The debris zones were mainly composed of various types of materials, including abandoned bamboo and fishing nets, plastics, glass bottles and other organic matter (Figure 2H). The debris zones are distributed in band-like patterns and generally parallel to the saltmarsh edge. However, the edges of the debris bands were not strictly straight, resulting in spatial inconsistency in the width. In this study, relatively straight portions were selected to define the boundaries of debris bands, and the distance between them was used to determine the width of the debris bands. In the north area of the saltmarsh, there were three obvious debris bands (DB) in December 2020. DB1 was located closest to the landward side, with a width of approximately 12 meters. The main debris material in DB1 was bamboo, forming a meandering band. Because of the different primary waste materials, the other area with marine debris was divided into DB2 and DB3. DB2 was primarily composed of marine debris and had a width of approximately 16 meters. DB3 was mainly comprised of organic matter, with the widest width of

about 37 meters. The organic matter included marsh plant litter, eroded plant stems and grass from sea or river (Figure 2E). In terms of the alongshore length of the debris bands, DB1 traverses the entire northern saltmarsh, while DB2 and DB3 gradually narrow and deflect toward the sea as they get closer to the northern side (Figure 2A). In March 2021, the width and length of DB1 remained relatively constant without obvious changes. There was little debris and plant litter left at the original location of DB2 and DB3, but a new debris band, DB4, occurred adjacent to DB1. DB4 was also composed of debris and plant litter, with a smaller width of 21 m compared with DB2 and DB3 (Figure 2F). Another difference between DB4 and DB2/DB3 was that DB4 traversed the entire northern saltmarsh without large width change (Figure 2B). In July 2021, the width of DB1 decreased to 8m because of the expansion of the nearby marsh, with plants growing between the bamboo debris. DB4 also narrowed from 21 m to 10 m but mainly because large plant clusters grew in the original plant litter area. There was also a new debris band (DB5) formed, 7m wide, with relatively less debris and much closer to the sea compared with other bands (Figure 2G). These three bands not only exhibited similar widths but also had comparable alongshore lengths. The northern portions of both DB1 and DB4 had finally become incorporated into the saltmarsh. (Figure 2C).

Inside the saltmarsh, there was another kind of special zone without, or with very few, plants, which we here defined as the unvegetated zone (UZ). Different from debris bands, the shape and distribution of the blank areas were more irregular, a rectangle encompassing the majority of the unvegetated area was selected as the boundary of the UZ, and its dimensions were considered as the length and width of the UZ (e.g., UZ1 in Figure 3E). In December 2020, an unvegetated zone (UZ1) was present near DB1, approximately 6 meters wide and 41 meters long (Figure 2E). UZ1 remained the same in March 2021, but a new unvegetated

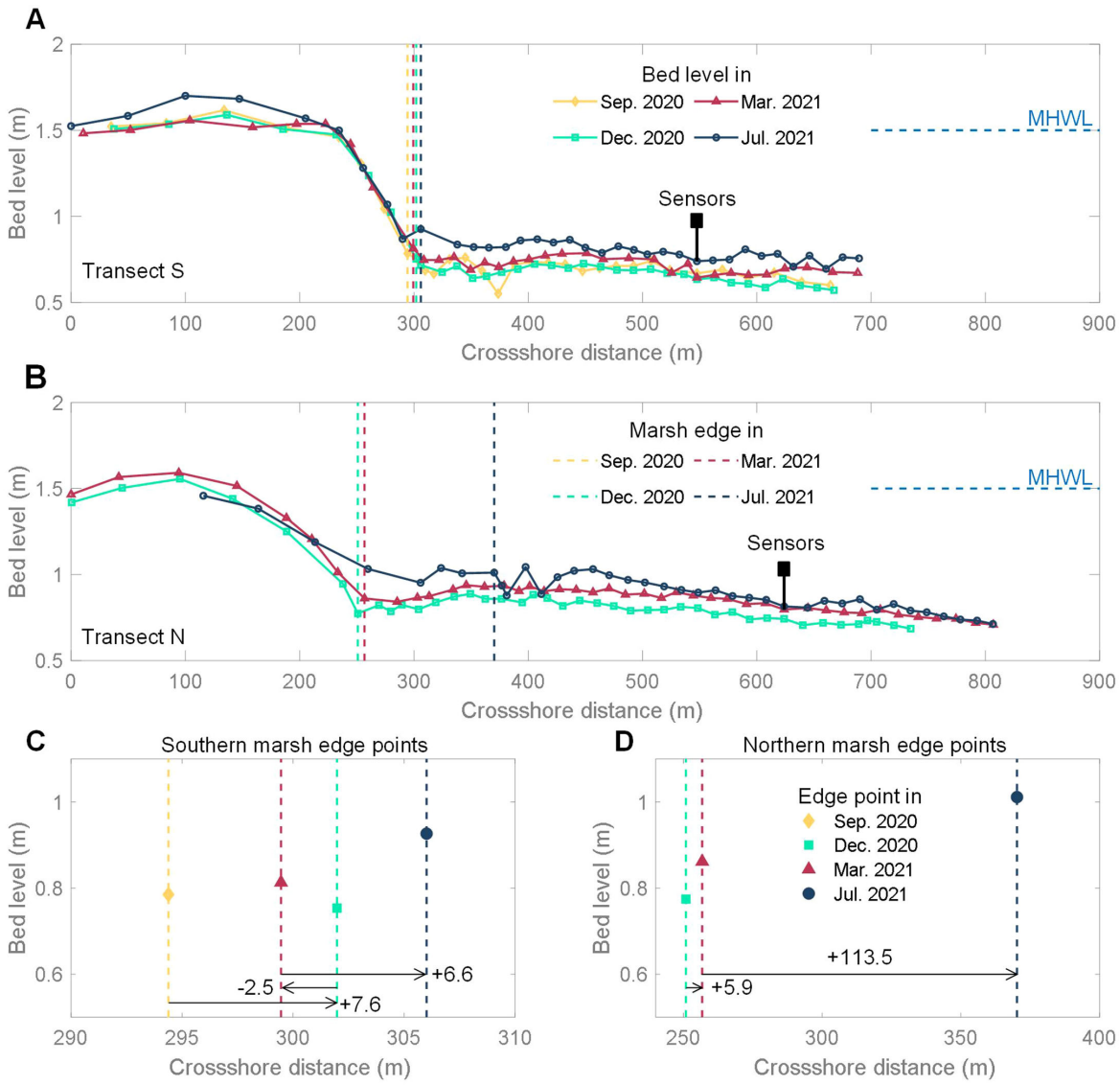

FIGURE 3
Bed level change of the transect S **(A)** and the transect N **(B)**. Marsh edge points shift of the transect S **(C)** and the transect N **(D)**.

zone (UZ2) appeared, which was band-like and located closer to the marsh edge (Figure 2F). In July 2021, the size of UZ1 decreased to about 34 m × 5 m because of the growth of plants, but there was still no plant cluster inside the unvegetated zone. However, UZ2 disappeared in July, as it had become entirely vegetated by marsh plants (Figure 2G).

3.2 Variation of bed level and marsh edge shift

The cross-shore bed level changes of transect S and transect N both showed that there was an elevation difference between the marsh platform and the unvegetated flat, transitioning through a gentle slope (Figures 3A, B), placing both into the "smooth transition" type of saltmarsh-edge landscapes (Allen, 2000). However, they exhibited distinct evolutionary trends.

The southern marsh edge point shifted seaward by 7.6 m from September 2020 to December 2020, then retreated by 2.5 meters from December 2020 to March 2021, and subsequently shifted seaward again by 6.6 meters from March 2021 to July 2021 (Figure 3C). The movement distance between each season was less than 10 meters, indicating a gradual seaward expansion of the southern saltmarsh over annual time scales but with seasonal oscillation. The northern marsh edge point also shifted seaward, but the movement was much larger and the distance reached 113.5 m from March 2021 to July 2021 (Figure 3D). From December 2020 to July 2021, the vertical elevation of both the southern and northern edge points increased. The increase of the northern point (0.24m) was slightly greater than that of the southern point (0.17m).

The mean bed levels of the marsh platform and unvegetated flat were calculated to show the overall evolutionary trend (Figure 4). Due to the accuracy of 15 mm in the vertical elevation data, the results in Figure 4 that conflict with the accuracy were only used for reference to obtain a general trend. From September 2020 to December 2020, the southern marsh and unvegetated flat overall experienced erosion, with the mean bed level decreasing by 0.02 m. The southern marsh and unvegetated flat started to accrete in December 2020, but the overall accretion of the southern marsh was little (0.01 m). With respect to the northern area, the mean bed levels of the marsh and unvegetated flat overall increased, but there was a decrease of 0.25 m in the northern marsh from March 2021 to July 2021. Moreover, there was a difference of approximately 0.1 m between the northern and southern bare flats, which indicated the presence of a tiny alongshore slope from north to south in the study area.

3.3 Processes of wave and water level

Hydrodynamic parameters were measured at two fixed sites, considered representative of the southern and northern regions, respectively (Figure 5). The southern site recorded the significant wave height (Hs) for four seasons, with the maximum values being 0.41 m in September 2020, 0.32 m in December 2020, 0.25 m in March 2021, and 0.40 m in July 2021 (with maximum average wind speed), respectively. The northern Hs presented a similar trend, with the maximum values for the same respective time periods being 0.23 m in December 2020, 0.25 m in March 2021, and 0.42 m in July 2021, respectively. Hs in the north were thus smaller in winter, the same in spring, and slightly larger in summer than Hs in the south. Water depths above the wetland surface at the northern site were consistently lower than those at the southern site reflecting the higher northern bed levels.

It should be noted that the hydrodynamics data in this study was collected during neap tides, which may be weaker than that during spring tides. Thus, future research is required to gain extended data covering longer periods.

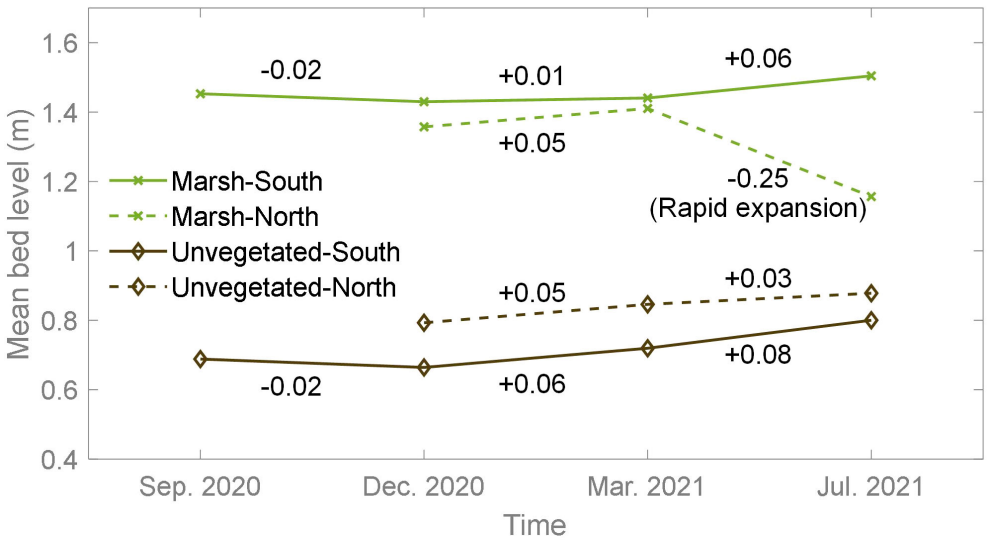

FIGURE 4
The mean bed level change of the marsh and unvegetated flat region.

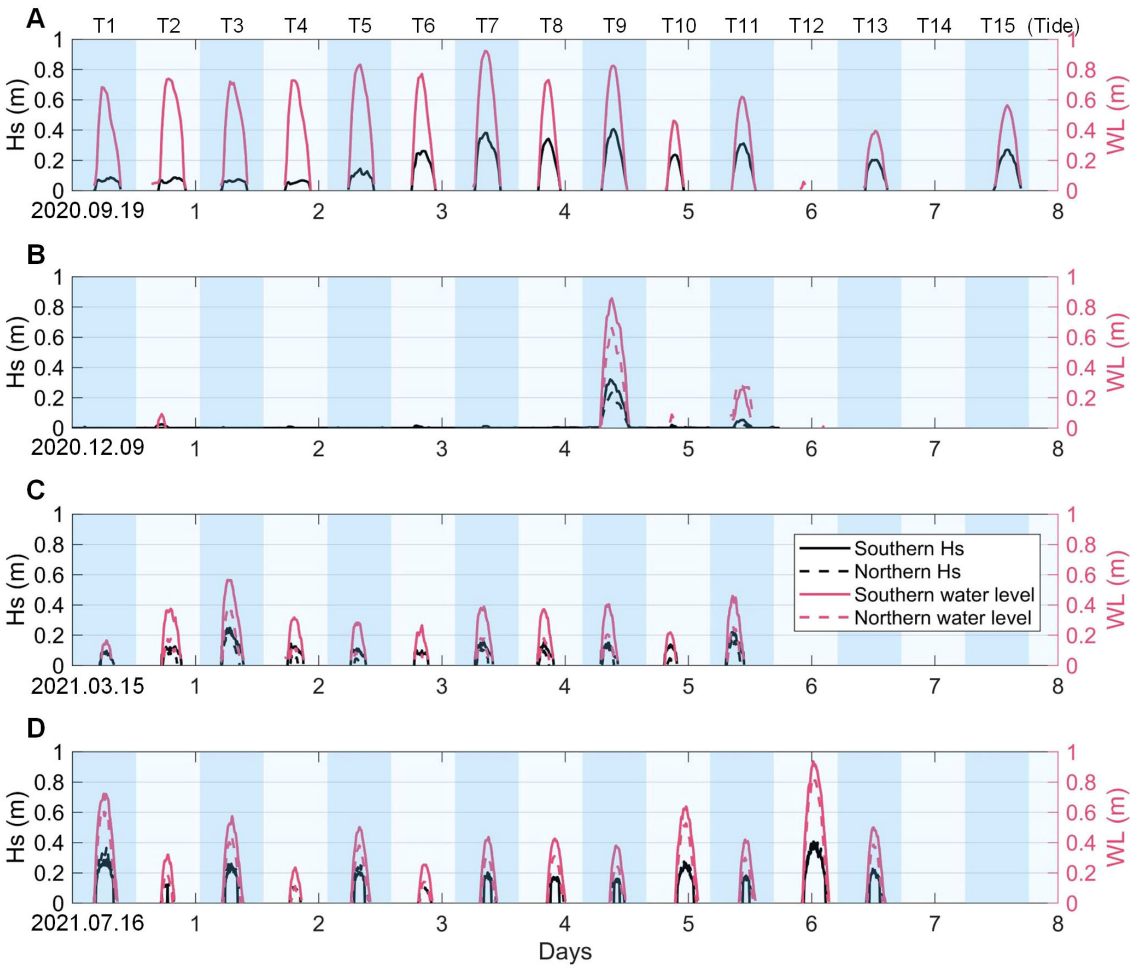

FIGURE 5
Significant wave height and water level of the southern and northern observation sites in 2020.09.19 **(A)**, 2020.12.09 **(B)**, 2021.03.15 **(C)** and 2021.07.16 **(D)**.

3.4 Distributions of vegetation and sediment

The above-ground biomass of *Spartina alterniflora* varied in a similar way along the cross-shore transects in both the southern and northern marsh (Figures 6A, B). Starting from the marsh edge, the distribution of southern biomass towards the land exhibited a bimodal pattern with two peaks and two troughs. The troughs were mainly distributed in the range of 120 - 170 m and 250 - 300 m (see Figure 3). The maximum biomass values for each season were 2.78 kg m^{-2} in autumn, 2.55 kg m^{-2} in summer, 2.21 kg m^{-2} in winter, and 1.63 kg m^{-2} in spring. However, the trough values were lowest in summer, 0.81 kg m^{-2} in Area S1 and 0.60 kg m^{-2} in Area S2 (Figure 6A). The seasonal differences were also reflected in the shifting range and position of the low-biomass zones, with the larger range observed in December 2020 (as shown by the dashed line range in Figure 6A). As mentioned above (section 3.1), these low-biomass zones were related to the debris bands and unvegetated zones, which were located inside the saltmarsh and whose position changed over time. The northern biomass distribution also showed the same mobile low-biomass zones. Because of the extensive seaward expansion of the northern marsh, a third new low-biomass zone appeared in July 2021 (Figure 6B). Moreover, the minimum biomass in March 2021 approached zero, indicating the presence of an unvegetated zone (e.g., UZ2 in Figure 2F).

The median sediment grain size near the marsh edge varied seasonally. At the southern edge point, the median grain size was 6.21 μm in summer, 7.77 μm in autumn, 12.30 μm in winter, and 12.86 μm in spring, indicating that the median grain size increased from summer to spring (Figure 6C). Meanwhile, the cross-shore distribution of the median grain size also showed zones of finer sediments, but located in different regions to the regions with low above-ground biomass. These particle-size lows were located more landward in September 2020, March 2021 and July 2021, while the lowest particle size in December 2020 was closer to the sea. The northern cross-shore distribution of median grain size exhibited a similar phenomenon, but its seasonal variation was more pronounced (Figure 6D).

In this study area, marine debris was observed to exhibit a band-like distribution in different regions, accompanied by seasonal

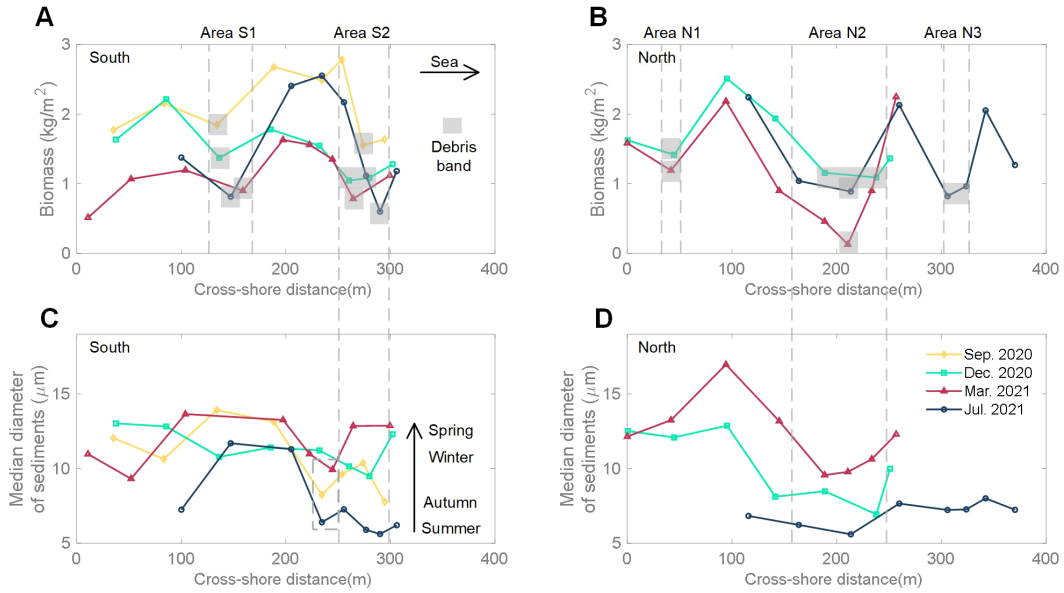

FIGURE 6
Biomass and median sediment grain size (D_{50}) in the marsh of transect S **(A, C)** and transect N **(B, D)**.

movements (Figure 2). From the biomass results (Figures 6A, B), it was evident that the presence of debris bands significantly reduced the biomass value in the adjacent area. If we assume that in the absence of debris bands, the vegetation biomass values for the corresponding area follow the linear interpolation between the seaward and landward values of the debris band, we can estimate the approximate percentage decrease in biomass due to the influence of debris bands (Figure 7). Biomass in Area S1 reduced from September 2020 to July 2021, representing 24% to 58% relative to the assumed fully vegetated state. The maximum decrease of biomass in Area S2 also occurred in July 2021, with a value of 48%. Overall, our results show that debris bands could result in a reduction of approximately 58% in biomass during the summer and around 30% during other seasons.

4 Discussion

4.1 Alongshore versus cross-shore expansion of saltmarsh patches

The lateral movement of the marsh edge has been a focal point of research (Bouma et al., 2016; Willemsen et al., 2018), as it plays a critical role in understanding and predicting the dynamic processes of marsh wetland evolution. Saltmarsh patches are often considered indicators of seaward accretion of the marsh edge. However, past research on this topic has predominantly focused on the cross-shore expansion pattern (Van der Wal et al., 2008), while the alongshore expansion pattern has been largely overlooked. This oversight could

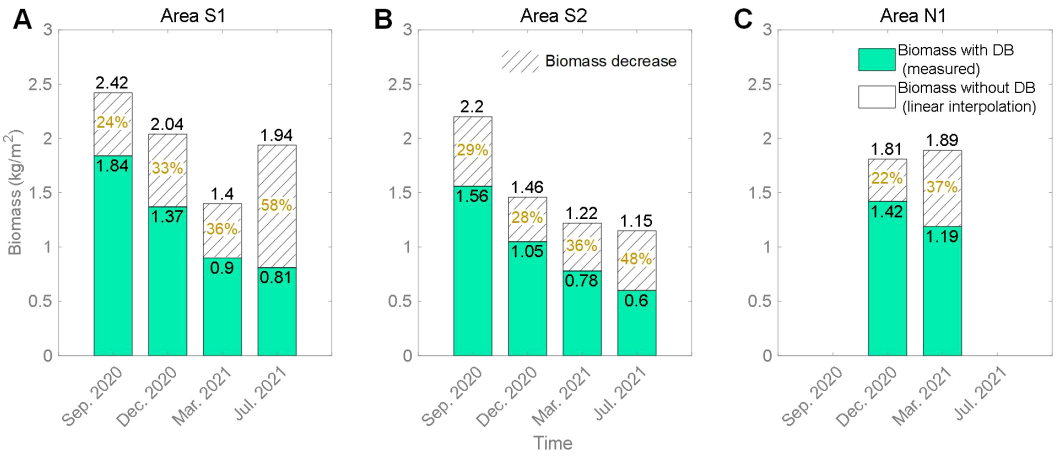

FIGURE 7
The percentage decrease of biomass due to the debris bands (DB) in Area S1 **(A)**, Area S2 **(B)** and Area N1 **(C)**. The "Area" corresponds to the region with debris bands in Figures 6A, B.

impact the accuracy of modelling and prediction of tidal wetland morphodynamics, as alongshore processes might contribute significantly to the alongshore morphological evolution of marshes.

Our study suggests that both alongshore and cross-shore expansion can occur at rates in excess of 100 m yr^{-1}, albeit in a spatially discontinuous fashion (UAV orthoimages): The marsh patches in the southern region followed a cross-shore dominated expansion pattern, i.e. the patch zone directly expanded seaward and patches then connected (Figure 2). The expansion rate was approximately 11.7 meters in one year (Figure 3C). In the northern region, marsh patches initially appeared on the northward unvegetated flat (Figure 2A), connecting to each other in the subsequent growth cycle and merging with the landward vegetated marsh (Figure 2C). Meanwhile, new patch areas formed southward rather than seaward. Eventually, the northern saltmarsh advanced toward the sea but through a form of alongshore expansion. The characteristic of this expansion pattern was the sudden and rapid seaward advancement of the marsh edge, with an alongshore expansion rate of approximately 180 m and a cross-shore expansion rate of approximately 119.4 m in one year, which also resulted in a sudden decrease in the mean elevation of the marsh edge (Figure 4). During the expansion process in the northern saltmarsh, there was a significant difference in the expansion rates between December 2020 to March 2021 and March 2021 to July 2021, which were 5.9 meters and 113.5 meters, respectively. This difference is related to the growth pattern of *Spartina alterniflora*, whose seeds can remain dormant until germination in the following spring, resulting in the rapid expansion observed between March 2021 and July 2021. Overall, both patterns achieved the seaward expansion of the saltmarsh, but alongshore spreading of patches with subsequent connection was critical in achieving the fast (> 100 m yr^{-1}) expansion rate.

What are the causes of the alongshore expansion? From Apr. 2017 to July 2018, Dai et al. (2021) conducted field observations in the same study area and found that both the southern and northern marsh edges expanded gradually seaward but not with any alongshore pattern. But in September 2020, a well-developed saltmarsh with vegetated protrusions onto the tidal flat was observed in the northern region (Figure 2A), which would have provided seeds for the subsequent development of patches towards the south. Our measurements show that alongshore currents in the northern area may have played a critical role in this expansion history (Figure 8): the alongshore current predominantly flowed southward with a maximum velocity of 0.26 m s^{-1} in March 2021 (spring), which would have facilitated the transport of vegetation seeds towards the south (Figure 8C). In July 2021 (summer), the alongshore current reversed to a northward dominant flow with a maximum velocity of 0.34 m s^{-1}, exceeding that in spring (Figure 8D). The strong north-westward flow during summer may have caused the edge of the newly developed marsh patch region to form at an angle with the shoreline (Figure 2C). The cross-shore current in spring and summer both predominantly flowed westward, with a maximum velocity of 0.23 m s^{-1} (Figures 8C, D), which may have limited the direct seaward expansion of plant seeds. The alongshore characteristics of the current near the marsh edge and the seasonal changes in the current direction were consistent with previous observations (Zhao et al., 2014). After July 2021, the marsh patches continued to grow and interconnected, completing their establishment (Supplementary Figure 1A). Moreover, although the subsequent alongshore current shifted to the north, the marsh

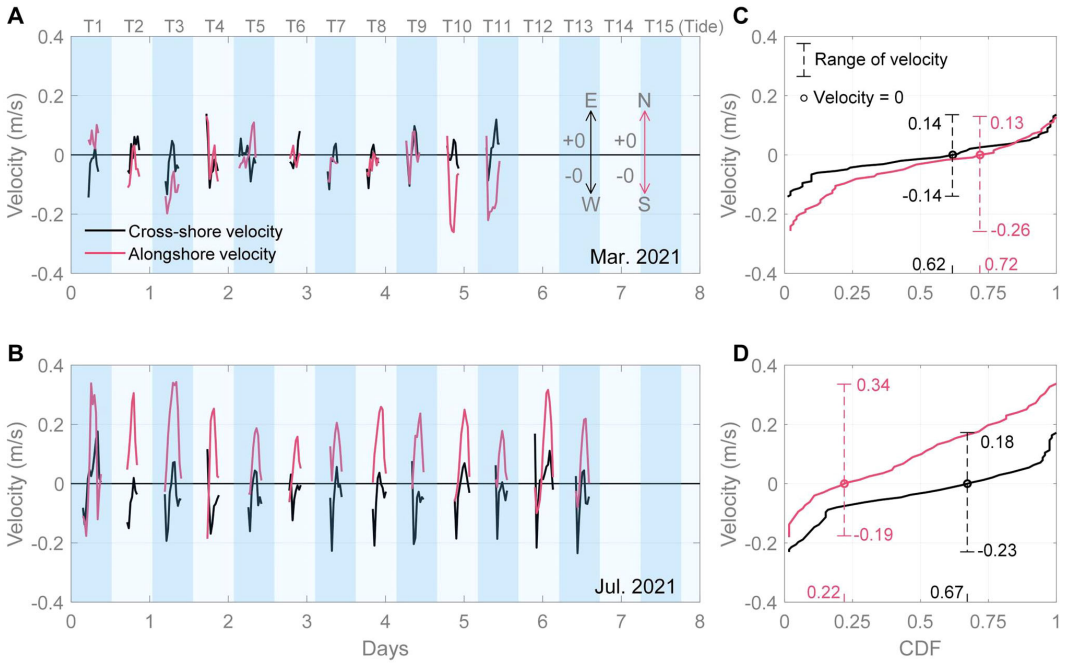

FIGURE 8
The current velocity and the cumulative distribution function (CDF) of velocity at the northern observation site in 2021.03.15 **(A, C)** and 2021.07.16 **(B, D)**. The current velocity data was sampled from a single layer located 0.15 m above the seabed.

remained relatively stable with minimal changes (Supplementary Figure 1B). We hypothesize that there are potentially two primary factors contributing to the formation of this alongshore saltmarsh expansion pattern: a well-developed initial saltmarsh area with protruding shorelines on which a strong alongshore current was able to act and facilitate expansion through the transport of sediment and seeds.

More detailed field sampling would elucidate whether this hypothesis holds here and potentially elsewhere. What is clear, however, is that, when considering the past and future evolution of an alongshore current dominated saltmarsh, this rapid alongshore saltmarsh expansion cannot be overlooked, especially in the context of the need to predict future saltmarsh areas for conservation and ecosystem service provision on comparably large, open coast settings.

4.2 Temporal variation of sediment grain size and vegetation biomass

Numerous studies have shown that saltmarshes can directly capture suspended sediment particles through locally enhancing salinity and particle flocculation or promoting sediment deposition by attenuating hydrodynamic (tidal or wave-induced flow) energy, hence facilitating the sediment settling processes (Yang, 1999; Mudd et al., 2010; Zhou et al., 2022a). Field observations on several tidal flats worldwide suggest that the sediment grain size exhibits a 'landward fining' phenomenon (Friedrichs, 2011), which indicates that saltmarshes mainly promote the deposition of the finer sediment. Some studies find that high magnitude tide/wave events (storms) can erode and suspend relatively coarse sediments on the lower flat, which can be transported shoreward and settle on the saltmarsh (Zhou et al., 2022b; Pannozzo et al., 2023) and, to some extent, changes the 'landward fining' trend. Yang (1999) mentioned that sediment grain size in the marsh area was also influenced by the seasonal changes in the vegetation.

In this study, the mean biomass of *Spartina alterniflora* shown in Figure 9 presented seasonal variation consistent with its biological growth characteristics. The distribution curve of the mean biomass exhibited a concave pattern from September 2020 to July 2021, with the minimum value occurring in March 2021 (spring). However, the trend of the mean D_{50} varies inversely with the mean biomass, which increased from September 2020 to March 2021 and then decreased, forming a convex curve (Figure 9). This indicated that the seasonal variation trend of sediment grain size in saltmarshes was opposite to the trend of vegetation biomass. The presence of vegetation facilitates the deposition of fine sediment particles, but with the seasonal weakening of vegetation capacity (i.e., winter), there is a trend of surface sediment coarsening in the saltmarsh area. Although geotechnical properties are affected by multiple factors (e.g., seasonal change in hydrodynamics) and need further investigation (Evans et al., 2022), this preliminary seasonal relationship between grain size and biomass can provide more specific evidence for the relatively simple biological processes in current bio-morphodynamic models, facilitating model development.

4.3 Spatial variation of vegetation biomass under the impact of marine debris

The spatial variation of Spartina biomass is influenced by various natural factors such as inundation duration, sea-level rise, storms, tidal creeks, marsh-edge morphology and so on (Mudd et al., 2004; Belliard et al., 2016; Chen et al., 2020b; Tang et al., 2022; Hang et al., 2024). Since inundation duration is the primary factor, biomass generally exhibits a parabolic distribution in the cross-shore direction (Morris et al., 2002; Mudd et al., 2004), which is the biomass distribution pattern used in most current bio-morphodynamic models (Zhou et al., 2016; Mariotti, 2020). In our study, however, we found that debris bands significantly impact the spatial distribution of vegetation biomass, which could result in a maximum reduction of approximately 58% in biomass (Figure 7). At this point, the traditional parabolic biomass distribution pattern becomes inapplicable, as it would significantly affect the accuracy of the surface growth component of marsh evolution models.

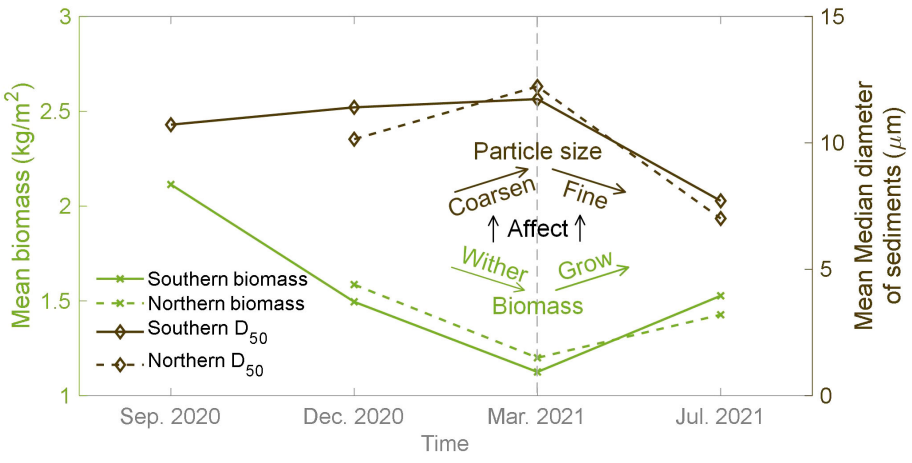

FIGURE 9
The seasonal variation of the mean vegetation biomass and the mean median diameter of sediment (D_{50}).

Further, our results showed that the debris bands were mobile (Figure 7) and that the location of the debris bands was determined by (as well as influenced) the seasonal variation of saltmarsh biomass with the latter likely determining the distance of the debris bands from the saltmarsh edge (i.e. debris more likely to be 'trapped' by areas of higher biomass).

By analyzing the movement and composition of debris bands, they could be classified into three main categories: stable type (e.g., DB1 in Figure 2), migrating type (e.g., DB2, DB4 and DB5 in Figure 2), and organic type (e.g., DB3 in Figure 2). The stable debris bands in our study were usually found in locations far from the saltmarsh edge, where they experienced minimal hydrodynamic influence. Thus, their location, width and length were less likely to change, which indicates that the influence of this kind of debris band on the underlying vegetation and soil is also likely to be longer lived. Compared to the stable type, the migrating debris bands were found closer to the marsh edge and were more susceptible to the action of waves and tides. The movement exhibited seasonal changes, likely because (a) the ability of vegetation to trap debris and (b) hydrodynamic conditions and thus their capacity to shift the material in the debris bands varied across seasons. Moreover, with the continuous seaward expansion of the saltmarsh, migrating debris bands might be expected to experience less disturbance over time and may potentially transform into the stable type (e.g., DB4 in Figure 2G). The organic debris band mainly consists of organic matter, such as plant litter and seaweed. These high-density organic materials were observed to form a dense matrix that was intricately connected to plant-standing crops. Coupled with the anaerobic conditions during decomposition, the tight 'interweaving' of the organic material with the marsh could make these debris bands significant determinants of marsh functioning and morphological evolution.

Currently, there is limited research on the interactions between debris bands and biogeomorphology, and the processes and mechanisms involved remain unclear. Our study clearly highlights that further in-depth research is warranted.

5 Conclusions

Our multi-method biogeomorphological field study on the open coast tidal marsh wetlands in Jiangsu, China, enabled us to build a more comprehensive picture of biogeomorphological processes over seasonal to annual time scales that have thus far been neglected in the tidal wetland literature. Our results revealed particularly that biophysical interactions among multiple processes could lead to previously overlooked sedimentary behaviors and bio-morphological patterns: Firstly, we observed that the dominance of alongshore currents facilitated an alongshore expansion of saltmarsh patches. Different from the commonly reported cross-shore expansion, the alongshore pattern achieved seaward advancement of the marsh edge by first alongshore spreading and then connecting, with an alongshore rate of approximately 180 m and a seaward rate of approximately 120 m in one year. Secondly, seasonally varying saltmarsh biomass coincided with seasonally varying sediment deposition, resulting in the particle size of sediment near the marsh edge coarsening when plants withered and fining when plants grew, with likely, as yet unexplored implications for soil ecology and stability. Thirdly, the interaction between vegetation and stranded marine debris formed banded debris zones within the saltmarsh. Results showed that debris bands could cause a biomass reduction of up to 58% during summer and around 30% during other seasons, altering the commonly observed parabolic biomass-elevation relationship in mono-specific Spartina wetlands. Meanwhile, the position of debris bands was affected by the seasonal variation of saltmarsh biomass and distance from the saltmarsh edge, suggesting that there is a feedback between the effect of the debris bands on vegetation and, in turn, of the vegetation on the likely future trapping of debris.

We challenge the developers of numerical morphodynamic models of saltmarsh evolution and those involved in saltmarsh management to consider the combination of quantitative and qualitative observations and relationships we have identified in this study. There is a clear case to be made for future studies that focus in more detail on the importance of these previously overlooked biophysical relationships.

Data availability statement

The original contributions presented in the study are included in the article/Supplementary Material. Further inquiries can be directed to the corresponding author.

Author contributions

LC: Conceptualization, Data curation, Investigation, Methodology, Writing – original draft, Writing – review & editing. IM: Conceptualization, Methodology, Resources, Supervision, Writing – review & editing. ZZ: Conceptualization, Funding acquisition, Methodology, Project administration, Resources, Supervision, Writing – review & editing. ZH: Methodology, Writing – review & editing. YZ: Resources, Writing – review & editing. MC: Resources, Writing – review & editing. YJ: Methodology, Writing – review & editing. IT: Conceptualization, Methodology, Writing – review & editing. CZ: Conceptualization, Funding acquisition, Methodology, Project administration, Resources, Supervision, Writing – review & editing.

Funding

The author(s) declare financial support was received for the research, authorship, and/or publication of this article. This study is supported by the National Key R&D Program of China (2022YFC3106201), the National Natural Science Foundation of China (NSFC, Grant Nos. 42361144873, 42376161), Carbon Peak & Carbon Neutral Science and Technology Innovation Project of

Jiangsu Province (BK20220020), Yellow Sea Wetlands Project (HHSDKT202306), the fund of National Key Laboratory of Water Disaster Prevention (Grant Nos. 5240152K2), and the Postgraduate Research & Practice Innovation Program of Jiangsu Province (KYCX20_0480).

Conflict of interest

The authors declare that the research was conducted in the absence of any commercial or financial relationships that could be construed as a potential conflict of interest.

The author(s) declared that they were an editorial board member of Frontiers, at the time of submission. This had no impact on the peer review process and the final decision.

Publisher's note

Supplementary material

The Supplementary Material for this article can be found online at: https://www.frontiersin.org/articles/10.3389/fmars.2024.1469307/full#supplementary-material

References

Allen, J. (2000). Morphodynamics of Holocene salt marshes: A review sketch from the Atlantic and Southern North Sea coasts of Europe. *Quat Sci. Rev.* 19, 1155–1231. doi: 10.1016/S0277-3791(99)00034-7

Barbier, E. B., Hacker, S. D., Kennedy, C., Koch, E. W., Stier, A. C., and Silliman, B. R. (2011). The value of estuarine and coastal ecosystem services. *Ecol. Monogr.* 81, 169–193. doi: 10.1890/10-1510.1

Belliard, J. P., Di Marco, N., Carniello, L., and Toffolon, M. (2016). Sediment and vegetation spatial dynamics facing sea-level rise in microtidal salt marshes: Insights from an ecogeomorphic model. *Adv. Water Resour* 93, 249–264. doi: 10.1016/j.advwatres.2015.11.020

Best, Ü.S.N., van der Wegen, M., Dijkstra, J., Willemsen, P. W. J. M., Borsje, B. W., and Roelvink, D. J. A. (2018). Do salt marshes survive sea level rise? Modelling wave action, morphodynamics and vegetation dynamics. *Environ. Model. Soft* 109, 152–166. doi: 10.1016/j.envsoft.2018.08.004

Bouma, T. J., van Belzen, J., Balke, T., van Dalen, J., Klaassen, P., Hartog, A. M., et al. (2016). Short-term mudflat dynamics drive long-term cyclic salt marsh dynamics. *Limnol Oceanogr* 61, 2261–2275. doi: 10.1002/lno.10374

Browne, M. A., Chapman, M. G., Thompson, R. C., Amaral Zettler, L. A., Jambeck, J., and Mallos, N. J. (2015). Spatial and temporal patterns of stranded intertidal marine debris: is there a picture of global change? *Environ. Sci. Technol.* 49, 7082–7094. doi: 10.1021/es5060572

Cao, Z., Zhang, Y., Wolfram, P. J., Brus, S. R., Rowland, J. C., Xu, C., et al. (2021). Effects of different vegetation drag parameterizations on the tidal propagation in coastal marshlands. *J. Hydrol (Amst)* 603, 126775. doi: 10.1016/j.jhydrol.2021.126775

Chen, C., Zhang, C., Schwarz, C., Tian, B., Jiang, W., Wu, W., et al. (2022). Mapping three-dimensional morphological characteristics of tidal salt-marsh channels using UAV structure-from-motion photogrammetry. *Geomorphology* 407, 108235. doi: 10.1016/j.geomorph.2022.108235

Chen, L., Zhou, Z., Xu, F., Jimenez, M., Tao, J., and Zhang, C. (2020a). Simulating the impacts of land reclamation and de-reclamation on the morphodynamics of tidal networks. *Anthropocene Coasts* 3, 30–42. doi: 10.1139/anc-2019-0010

Chen, L., Zhou, Z., Xu, F., Möller, I., and Zhang, C. (2020b). Field observation of saltmarsh-edge morphology and associated vegetation characteristics in an open-coast tidal flat.s. *J. Coast. Res.* 95, 412–416. doi: 10.2112/SI95-080.1

Chung, C. H., Zhuo, R. Z., and Xu, G. W. (2004). Creation of Spartina plantations for reclaiming Dongtai, China, tidal flats and offshore sands. *Ecol. Eng.* 23, 135–150. doi: 10.1016/j.ecoleng.2004.07.004

Corbau, C., Buoninsegni, J., Olivo, E., Vaccaro, C., Nardin, W., and Simeoni, U. (2023). Understanding through drone image analysis the interactions between geomorphology, vegetation and marine debris along a sandy spit. *Mar. Pollut. Bull.* 187, 114515. doi: 10.1016/j.marpolbul.2022.114515

Dai, W., Li, H., Gong, Z., Zhou, Z., Li, Y., Wang, L., et al. (2021). Self-organization of salt marsh patches on mudflats: Field evidence using the UAV technique. *Estuar. Coast. Shelf Sci.* 262, 107608. doi: 10.1016/j.ecss.2021.107608

Evans, B. R., Brooks, H., Chirol, C., Kirkham, M. K., Möller, I., Royse, K., et al. (2022). Vegetation interactions with geotechnical properties and erodibility of salt marsh sediments. *Estuar. Coast. Shelf Sci.* 265, 107713. doi: 10.1016/j.ecss.2021.107713

Fraaije, R. G. A., Braak, C. J. F., Verduyn, B., Breeman, L. B. S., Verhoeven, J. T. A., and Soons, M. B. (2015). Early plant recruitment stages set the template for the development of vegetation patterns along a hydrological gradient. *Funct. Ecol.* 29, 971–980. doi: 10.1111/1365-2435.12441

Frazier, P., and Page, K. (2000). Water body detection and delineation with Landsat TM data. *Photogramm Eng. Remote Sens.* 66, 1461–1467.

Friedrichs, C. T. (2011). Tidal flat morphodynamics: A synthesis. *Treatise Estuar. Coast. Sci.* 3, 137–170. doi: 10.1016/B978-0-12-374711-2.00307-7

Gao, S., Du, Y., Xie, W., Gao, W., Wang, D., and Wu, X. (2014). Environment-ecosystem dynamic processes of Spartina alterniflora salt-marshes along the eastern China coastlines. *Sci. China Earth Sci.* 57, 2567–2586. doi: 10.1007/s11430-014-4954-9

Hang, J., Gong, Z., Jin, C., and Li, H. (2024). Biomass distribution patterns of salt marshes: A detailed spatial analysis in central China's coastal wetlands. *Ocean Coast. Manag* 254, 107212. doi: 10.1016/j.ocecoaman.2024.107212

Houttuijn Bloemendaal, L. J., FitzGerald, D. M., Hughes, Z. J., Novak, A. B., and Phippen, P. (2021). What controls marsh edge erosion? *Geomorphology* 386, 107745. doi: 10.1016/J.GEOMORPH.2021.107745

Li, J., Yan, D., Yao, X., Liu, Y., Xie, S., Sheng, Y., et al. (2022). Dynamics of carbon storage in saltmarshes across China's eastern coastal wetlands from 1987 to 2020. *Front. Mar. Sci.* 9. doi: 10.3389/fmars.2022.915727

Li, S. H., Ge, Z. M., Xin, P., Tan, L. S., Li, Y. L., and Xie, L. N. (2021). Interactions between biotic and abiotic processes determine biogeomorphology in Yangtze Estuary coastal marshes: Observation with a modeling approach. *Geomorphology* 395, 107970. doi: 10.1016/j.geomorph.2021.107970

Li, X., Bellerby, R., Craft, C., and Widney, S. E. (2018). Coastal wetland loss, consequences, and challenges for restoration. *Anthropocene Coasts* 1, 1–15. doi: 10.1139/anc-2017-0001

Li, X., Leonardi, N., and Plater, A. J. (2019). Wave-driven sediment resuspension and salt marsh frontal erosion alter the export of sediments from macro-tidal estuaries. *Geomorphology* 325, 17–28. doi: 10.1016/j.geomorph.2018.10.004

Marani, M., Belluco, E., Ferrari, S., Silvestri, S., D'Alpaos, A., Lanzoni, S., et al. (2006). Analysis, synthesis and modelling of high-resolution observations of salt-marsh eco-geomorphological patterns in the Venice lagoon. *Estuar. Coast. Shelf Sci.* 69, 414–426. doi: 10.1016/j.ecss.2006.05.021

Mariotti, G. (2020). Beyond marsh drowning: The many faces of marsh loss (and gain). *Adv. Water Resour* 144, 103710. doi: 10.1016/j.advwatres.2020.103710

Moffett, K., Nardin, W., Silvestri, S., Wang, C., and Temmerman, S. (2015). Multiple stable states and catastrophic shifts in coastal wetlands: progress, challenges, and opportunities in validating theory using remote sensing and other methods. *Remote Sens (Basel)* 7, 10184–10226. doi: 10.3390/rs70810184

Möller, I. (2006). Quantifying saltmarsh vegetation and its effect on wave height dissipation: Results from a UK East coast saltmarsh. *Estuar. Coast. Shelf Sci.* 69, 337–351. doi: 10.1016/j.ecss.2006.05.003

Möller, I., Kudella, M., Rupprecht, F., Spencer, T., Paul, M., van Wesenbeeck, B. K., et al. (2014). Wave attenuation over coastal salt marshes under storm surge conditions. *Nat. Geosci* 7, 727–731. doi: 10.1038/ngeo2251

Morris, J. T., Sundareshwar, P. V., Nietch, C. T., Bjo¨, B., Kjerfve, B., and Cahoon, A. D. R. (2002). Responses of coastal wetlands to rising sea level. *Ecology* 83, 2869–2877. doi: 10.1890/0012-9658(2002)083

Mudd, S. M., D'Alpaos, A., and Morris, J. T. (2010). How does vegetation affect sedimentation on tidal marshes? Investigating particle capture and hydrodynamic controls on biologically mediated sedimentation. *J. Geophys Res.* 115, F03029–F03029. doi: 10.1029/2009JF001566

Mudd, S. M., and Fagherazzi, S. (2016). "Salt marsh ecosystems: tidal flow, vegetation, and carbon dynamics," in *A Biogeoscience Approach to Ecosystems*. Eds. E. A. Johnson and Y. E. Martin (Cambridge University Press, Cambridge), 407–434. Available at: https://www.cambridge.org/core/books/biogeoscience-approach-to-ecosystems/salt-marsh-ecosystems-tidal-flow-vegetation-and-carbon-dynamics/663CD8CA3A72D1E7D1D9B0639F2353AF.

Mudd, S. M., Fagherazzi, S., Morris, J. T., and Furbish, D. J. (2004). "Flow, sedimentation, and biomass production on a vegetated salt marsh in south carolina: toward a predictive model of marsh morphologic and ecologic evolution," in *The Ecogeomorphology of Tidal Marshes*, 165–188. doi: 10.1029/CE059p0165

Nahlik, A. M., and Fennessy, M. S. (2016). Carbon storage in US wetlands. *Nat. Commun.* 7, 1–9. doi: 10.1038/ncomms13835

Pannozzo, N., Leonardi, N., Carnacina, I., and Smedley, R. (2021). Salt marsh resilience to sea-level rise and increased storm intensity. *Geomorphology* 389, 107825. doi: 10.1016/j.geomorph.2021.107825

Pannozzo, N., Leonardi, N., Carnacina, I., and Smedley, R. K. (2023). Storm sediment contribution to salt marsh accretion and expansion. *Geomorphology* 430, 108670. doi: 10.1016/j.geomorph.2023.108670

Spencer, T., Schuerch, M., Nicholls, R. J., Hinkel, J., Lincke, D., Vafeidis, A. T., et al. (2016). Global coastal wetland change under sea-level rise and related stresses: The DIVA Wetland Change Model. *Glob Planet Change* 139, 15–30. doi: 10.1016/j.gloplacha.2015.12.018

Tang, Y.-N., Ma, J., Xu, J.-X., Wu, W.-B., Wang, Y.-C., Guo, H.-Q., et al. (2022). Assessing the impacts of tidal creeks on the spatial patterns of coastal salt marsh vegetation and its aboveground biomass. *Remote Sens.* 14, 1839. doi: 10.3390/rs14081839

Thiel, M., Hinojosa, I. A., Miranda, L., Pantoja, J. F., Rivadeneira, M. M., and Vásquez, N. (2013). Anthropogenic marine debris in the coastal environment: A multi-year comparison between coastal waters and local shores. *Mar. pollut. Bull.* 71, 307–316. doi: 10.1016/j.marpolbul.2013.01.005

Uhrin, A. V., and Schellinger, J. (2011). Marine debris impacts to a tidal fringing-marsh in North Carolina. *Mar. Pollut. Bull.* 62, 2605–2610. doi: 10.1016/j.marpolbul.2011.10.006

van de Koppel, J., van der Wal, D., Bakker, J. P., and Herman, P. M. J. (2005). Self-organization and vegetation collapse in salt marsh ecosystems. *Am. Nat.* 165, E1–E12. doi: 10.1086/426602

van der Wal, D., van Dalen, J., Willemsen, P. W. J. M., Borsje, B. W., and Bouma, T. (2023). Gradual versus episodic lateral saltmarsh cliff erosion: Evidence from Terrestrial Laser Scans (TLS) and Surface Elevation Dynamics (SED) sensors. *Geomorphology* 426, 108590. doi: 10.1016/j.geomorph.2023.108590

Van der Wal, D., Wielemaker-Van den Dool, A., and Herman, P. M. J. (2008). Spatial patterns, rates and mechanisms of saltmarsh cycles (Westerschelde, The Netherlands). *Estuar. Coast. Shelf Sci.* 76, 357–368. doi: 10.1016/j.ecss.2007.07.017

Viehman, S., Vander Pluym, J. L., and Schellinger, J. (2011). Characterization of marine debris in North Carolina salt marshes. *Mar. pollut. Bull.* 62, 2771–2779. doi: 10.1016/j.marpolbul.2011.09.010

Wei, W., Dai, Z., Pang, W., Wang, J., Chen, Y., and Gao, S. (2022). Frequency-dependent wave damping by tidal wetlands under storm conditions. *J. Hydrol. (Amst)* 613, 128415. doi: 10.1016/j.jhydrol.2022.128415

Willemsen, P. W. J. M., Borsje, B. W., Hulscher, S. J. M. H., van der Wal, D., Zhu, Z., Oteman, B., et al. (2018). Quantifying bed level change at the transition of tidal flat and salt marsh: can we understand the lateral location of the marsh edge? *J. Geophys Res. Earth Surf.* 123, 2509–2524. doi: 10.1029/2018JF004742

Wu, W., Zhou, Y.x., and Tian, B. (2017). Coastal wetlands facing climate change and anthropogenic activities: A remote sensing analysis and modelling application. *Ocean Coast. Manag.* 138, 1–10. doi: 10.1016/j.ocecoaman.2017.01.005

Yang, S. L. (1999). Sedimentation on a Growing Intertidal Island in the Yangtze River Mouth. *Estuar. Coast Shelf Sci.* 49, 401–410. doi: 10.1006/ECSS.1999.0501

Yang, S. L., Fan, J. Q., Shi, B. W., Bouma, T. J., Xu, K. H., Yang, H. F., et al. (2019). Remote impacts of typhoons on the hydrodynamics, sediment transport and bed stability of an intertidal wetland in the Yangtze Delta. *J. Hydrol. (Amst)* 575, 755–766. doi: 10.1016/j.jhydrol.2019.05.077

Zhang, R. S., Shen, Y. M., Lu, L. Y., Yan, S. G., Wang, Y. H., Li, J. L., et al. (2004). Formation of Spartina alterniflora salt marshes on the coast of Jiangsu Province, China. *Ecol. Eng.* 23, 95–105. doi: 10.1016/j.ecoleng.2004.07.007

Zhao, Y., Gao, S., Wang, D., Xu, Z., Zhu, D., and Wang, X. (2014). Characteristics and formation mechanisms of the rhythmic morphology of salt-marsh edge cliffs. *Dili Xuebao/Acta Geograph Sin.* 69, 378–390. doi: 10.11821/dlxb201403009

Zhao, Y., Yu, Q., Wang, D., Wang, Y. P., Wang, Y., and Gao, S. (2017). Rapid formation of marsh-edge cliffs, Jiangsu coast, China. *Mar. Geol.* 385, 260–273. doi: 10.1016/j.margeo.2017.02.001

Zhou, Z., Liang, M., Chen, L., Xu, M., Chen, X., Geng, L., et al. (2022a). Processes, feedbacks, and morphodynamic evolution of tidal flat–marsh systems: Progress and challenges. *Water Sci. Eng.* 15, 89–102. doi: 10.1016/j.wse.2021.07.002

Zhou, Z., Wu, Y., Fan, D., Wu, G., Luo, F., Yao, P., et al. (2022b). Sediment sorting and bedding dynamics of tidal flat wetlands: Modeling the signature of storms. *J. Hydrol. (Amst)* 610, 127913. doi: 10.1016/j.jhydrol.2022.127913

Zhou, Z., Ye, Q., and Coco, G. (2016). A one-dimensional biomorphodynamic model of tidal flats: Sediment sorting, marsh distribution, and carbon accumulation under sea level rise. *Adv. Water Resour.* 93, 288–302. doi: 10.1016/j.advwatres.2015.10.011